Bull. Soc. R. Sci. Liège, 2024, **93**(2), 406–429 *Peer-reviewed conference paper*
doi:10.25518/0037-9565.11730

On the potential of Carbon–enhanced Metal-poor Stars for Galactic Archaeology

Aruna GOSWAMI[1,*], Jameela SHEJEELAMMAL[1,2], Partha Pratim GOSWAMI[1] and Meenakshi PURANDARDAS[1]

[1] Indian Institute of Astrophysics, Koramangala, Bangalore 560034, India
[2] Universidade de Sao Paulo, Instituto de Astronomia, Rua do Matao 1226, Cidade Universitaria, 05508-900, SP, Brazil
[*] Corresponding author: aruna@iiap.res.in

Paper presented at the 3rd BINA Workshop on "Scientific Potential of the Indo-Belgian Cooperation", held at the Graphic Era Hill University, Bhimtal (India), 22nd–24th March 2023.

Abstract

The low-mass metal-poor stars in the Galaxy that preserve in their atmosphere, the chemical imprints of the gas clouds from which they were formed can be used as probes to get insight into the origin and evolution of elements in the early galaxy, early star formation and nucleosynthesis. Among the metal-poor stars, a large fraction, the so-called carbon-enhanced metal-poor (CEMP) stars exhibits high abundance of carbon. These stars exhibit diverse abundance patterns, particularly for heavy elements, based on which they are classified into different groups. The diversity of abundance patterns points at different formation scenarios. Hence, accurate classification of CEMP stars and knowledge of their distribution is essential to understand the role and contribution of each group. While CEMP-s and CEMP-r/s stars can be used to get insight into binary interactions at very low metallicity, CEMP-no stars can be used to probe the properties of the first stars and early nucleosynthesis. To exploit the full potential of CEMP stars for Galactic archaeology a homogeneous analysis of each class is extremely important. Our efforts towards, and contributions to providing an improved classification scheme for accurate classification of CEMP-s and CEMP-r/s stars and in characterizing the companion asymptotic giant branch (AGB) stars of CH, CEMP-no, CEMP-s and CEMP-r/s binary systems are discussed. Some recent results obtained based on low- and high-resolution spectroscopic analysis of a large number of potential CH and CEMP star candidates are highlighted.

Keywords: Metal-Poor stars, Carbon stars, Nucleosynthesis, Abundances

1. Introduction

A number of large sky survey programs in the past, such as, HK survey (Beers et al., 1985, 1992, 2007; Beers, 1999), Hamburg/ESO Survey (HES; Christlieb et al. (2001a,b); Christlieb (2003); Christlieb et al. (2008)), Sloan Digital Sky Survey (SDSS; York et al. (2000)), LAMOST

(Large Sky Area Multi-Object Fiber Spectroscopic Telescope) survey (Cui et al., 2012; Deng et al., 2012; Zhao et al., 2012) were dedicated for identifying the most metal-poor stars. These surveys revealed that a significant fraction ($\sim$ 20% of Very Metal-Poor (VMP), [Fe/H] < -2) stars in the Galaxy are CEMP stars (Rossi et al., 1999; Christlieb, 2003; Lucatello et al., 2005, 2006; Carollo et al., 2012) and that the fraction of these stars increases with decreasing metallicity $\sim$ 40% for [Fe/H] < -3 and $\sim$ 75% for [Fe/H] < -4 (Yong et al., 2013a; Lee et al., 2013; Aoki et al., 2013; Placco et al., 2014; Frebel and Norris, 2015).

Beers and Christlieb (2005) first introduced four sub-classes of CEMP stars considering the abundances of carbon and two n-capture elements, Ba (a representative s-process element) and Eu (a representative r-process element). Subsequently, various authors (Jonsell et al., 2006; Masseron et al., 2010; Norris et al., 2010; Bisterzo et al., 2011; Bonifacio et al., 2015; Maeder and Meynet, 2015; Yoon et al., 2016; Abate et al., 2016; Hansen et al., 2016; Frebel, 2018; Hansen et al., 2019; Skúladóttir et al., 2020; Goswami et al., 2021) put forward different criteria for the identification and classification of the CEMP stars. The four primary sub-classes that are based on the level of relative enrichment of neutron-capture elements are: CEMP-s (shows enhanced abundances of s-process elements), CEMP-r (shows strong enhancement of r-process elements), CEMP-r/s (shows enhancement of both s- and r-process elements) and CEMP-no (does not show any enhanced abundance of neutron-capture elements). The diverse abundance patterns point at different formation scenarios for the respective sub-classes. The fractions and properties of CEMP sub-classes provide a unique opportunity to probe the formation and evolution of the Galactic halo and its building blocks. For this reason, the CEMP stars alongside the halo tracers CH stars have been extensively studied in the last few decades.

CH stars ($-2 \leq$ [Fe/H] ≤ -0.2) are characterized by strong CH and C_2 molecular bands, C/O > 1 and strong features due to the neutron-capture elements (Keenan, 1942). These are mostly high velocity objects ($V_r > 100\,\mathrm{km\,s^{-1}}$), and members of the Galactic halo. A few CH stars are also found in Globular clusters. Sub-giant CH stars have moderate velocities and they exhibit old disk behaviour rather than the halo. These objects are believed to be the progenitors of metal-deficient Ba stars. Long term radial velocity study by McClure and Woodsworth (1990) showed that most of the CH stars are binaries with companions that are now presumably white dwarfs. The heavy s-process elements in giant CH stars are found to be more enhanced than the light s-process elements (Karinkuzhi and Goswami, 2014, 2015), in agreement with theoretical modelling of s-process in stars and its dependence on the metallicity (Busso et al., 1999, 2001; Cristallo et al., 2016).

The CEMP-s stars are the metal-poor analogue of Ba and CH stars (Lucatello et al., 2005; Abate et al., 2016). A number of long-term radial velocity monitoring studies have shown that most of the CEMP-s stars are binaries (Lucatello et al., 2005; Starkenburg et al., 2014; Jorissen et al., 2016; Hansen et al., 2016), supporting the pollution from companion AGB stars. Comparisons of observed abundances in the CEMP-s stars with theoretical model predictions confirm the binary mass-transfer from the AGB companion (Bisterzo et al., 2011; Placco et al., 2013; Hollek et al., 2015; Shejeelammal et al., 2020; Shejeelammal and Goswami, 2021, 2022; Goswami et al., 2021; Goswami and Goswami, 2022).

The CEMP-r/s stars show abundance enhancement in both slow (s) and rapid (r) neutron capture process elements. Since most of the CEMP-r/s stars are also found to be binaries just like CEMP-s stars, binary mass transfer from the AGB companion is thought to be the reason for their origin as well, however the presence of r-process component posed a challenge (Jonsell et al., 2006; Herwig et al., 2011; Abate et al., 2016). It was proposed by Cowan and Rose (1977) that the intermediate neutron-capture process the so-called i-process, with neutron density between s- and r- process can produce both s- and r-process elements at a single stellar site. Many studies have successfully used model yields of i-process in low-mass low-metallicity AGB stars to account for the observed abundance patterns in CEMP-r/s stars (Hampel et al., 2016, 2019; Goswami et al., 2021; Shejeelammal et al., 2020; Shejeelammal and Goswami, 2021, 2022). Although there are several suggestions for the i-process sites, such as, super-massive AGB stars (Doherty et al., 2015; Jones et al., 2016), low-mass low-metallicity stars (Campbell and Lattanzio, 2008; Campbell et al., 2010; Cruz et al., 2013; Cristallo et al., 2016), and rapidly accreting white dwarfs (Herwig et al., 2014; Denissenkov et al., 2017) etc., the exact astrophysical site for the i-process is not yet confirmed (Frebel, 2018; Koch et al., 2019).

CEMP-r stars are extremely rare. In spite of several studies on the formation of CEMP-r stars, the origin of these stars are not yet clearly understood; observations of more such stars are required to constrain their exact origin.

The CEMP-no stars with enhanced carbon abundance and no signatures of heavy neutron-capture elements, are believed to be the most chemically primitive objects presently known (Norris and Yong, 2019; Yoon et al., 2020). These stars occupy the lowest metallicity tail ([Fe/H] < -3) of the Metallicity Distribution Function (MDF) of the Galaxy (Yong et al., 2013b; de Bennassuti et al., 2017; Yoon et al., 2019; Norris and Yong, 2019). Among the fourteen known CEMP stars with [Fe/H] < -4.5, twelve stars belong to the CEMP-no group. Being the oldest stars that can be directly observed at present, valuable information can be derived from them, such as the formation and nucleosynthesis pathways of the first stars, initial conditions for star and galaxy formation (Klessen et al., 2012; Frebel and Norris, 2015; Bonifacio et al., 2015; Hansen et al., 2016; Yoon et al., 2020, 2018), large galaxy assembly (e.g., Carollo et al. (2007)), and early nucleosynthesis (Hansen et al., 2011; Gil-Pons et al., 2021; Qian, 2022)). Further, these stars are expected to shed light on the physical processes resulting in the transitions from massive Population III (Pop III) stars to normal Population II (Pop II) stars (Salvadori et al., 2007; Hartwig et al., 2015; de Bennassuti et al., 2017).

Different scenarios have been suggested by various authors for the origin of CEMP-no stars (Hansen et al. (2015), Yoon et al. (2016) and references there in), however, the exact origin of these stars still remains unknown. According to some authors, the CEMP-no stars are generally single stars, suggesting an intrinsic origin, i.e., formed from a pre-enriched natal cloud of ISM (Spite et al., 2013; Starkenburg et al., 2014; Bonifacio et al., 2015; Hansen et al., 2016; Yoon et al., 2016). Suggested progenitors for the CEMP-no stars also include: (i) faint supernovae that underwent mixing and fall back (Umeda and Nomoto, 2003, 2005; Tominaga et al., 2014); (ii) extremely metal-poor fast rotating massive stars or spinstars that enriched the ISM with C, N, and O through strong stellar winds (Meynet et al., 2006; Frischknecht et al., 2012; Maeder

et al., 2015; Choplin et al., 2017); and (iii) i-process in massive Pop III stars (Clarkson et al., 2018). A recent study by Arentsen et al. (2019) has shown that the binary mass-transfer from an extremely metal-poor AGB companion could also be a possible progenitor of the CEMP-no stars. If the binary-mass-transfer scenario holds true for the origin of CEMP-no stars, this will help to understand extremely metal-poor AGB stars and provide robust observational constraints to the AGB nucleosynthesis and mass-transfer models for metallicity [Fe/H] < -2.

Since most of the metal-poor stars in the halo trace their origin to the dwarf satellite galaxies (Frebel and Norris, 2015; Frebel and Ji, 2023), they are ideal tools to study the Galactic halo assembly. Based on the kinematic, chemical, and dynamical properties of a sample of 644 CEMP stars, Zepeda et al. (2023) have shown that the CEMP-no stars are not in-situ to the Galaxy, but were originally born in satellite galaxies that were accreted and disrupted by the Milky Way. This is also in support of the findings of Yoon et al. (2019). Several authors have discussed the relevance and scope of enhancing medium- and high-resolution spectroscopic studies of different sub-groups of CEMP stars to further our understanding of early Galactic chemical evolution and Galactic halo formation (e.g., Hansen et al. (2015); Norris and Yong (2019); Yoon et al. (2019, 2020); Zepeda et al. (2023)). Along this line, we had conducted high-resolution spectroscopic studies of several potential CH and CEMP star candidates identified from low-resolution spectroscopic studies with the aim of deriving clues to their origin.

In Sect. 2, we discuss the limitations in classifying CEMP stars based on low-resolution spectra. Shortcomings of current classification criteria for CEMP-s and CEMP-r/s stars are discussed in Sect. 3. A revised classification scheme for identifying the CEMP-s and CEMP-r/s stars is also presented in this section. In Sect. 4, we discuss about characterizing the companion AGBs of the CH, CEMP-s and CEMP-r/s stars. A discussion on deriving clues for the origin of CEMP-r/s stars from abundance patterns is presented in Sect. 5. Observational evidence for multiple origins for CEMP-no stars is discussed in Sect. 6. The unique star HE 1005–1439 that shows evidence of occurrence of dual nucleosynthesis is discussed in Sect. 7. A few critical issues in the analysis of CEMP stars are discussed in Sect. 8. The conclusions are presented in Sect. 9.

2. Limitations in Classifying CEMP Stars Using Low-resolution Spectra

Due to the intrinsic weakness of the absorption features, using low-resolution samples, it is difficult to distinguish between different sub-classes of CEMP stars. This is illustrated in Fig. 1, where a few examples of low-resolution ($R \sim 1300$) spectra of CEMP stars obtained with HCT/HFOSC are shown.

Detail analysis of these spectra can be found in Goswami (2005) and Goswami et al. (2010). Visual inspection shows that the spectra look alike, and hence, it is difficult to identify if they belong to different sub-classes. The spectra are characterized by strong features of carbon molecules, and lines due to Ba and Sr are only marginally detectable. However, high resolution spectroscopic analyses have shown that HE 0319–0215 and HE 1305+0132 are CEMP-s stars and that HE 0017+0058 is a CEMP-r/s star (Goswami et al., 2021). Although the origin of

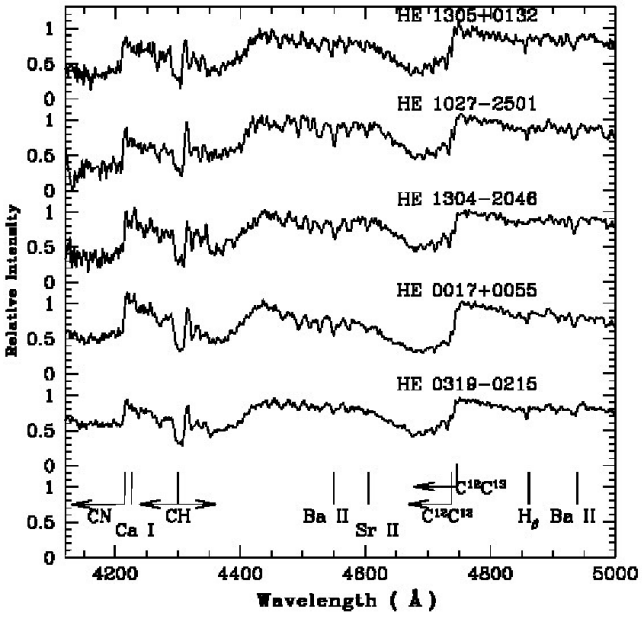

Figure 1: Low resolution ($R \sim 1300$) spectra of a few CEMP stars. The spectra characterized by strong carbon molecular features look alike and it is difficult to classify them into different CEMP sub-classes based on the low-resolution spectra. Follow-up high resolution spectroscopic studies have confirmed the objects HE 0319−0215 and HE 1305+0132 as CEMP-s stars and HE 0017+0058 as a CEMP-r/s star.

both these classes can be explained based on a binary picture with a now invisible white dwarf companion, the progenitors AGBs have very different nucleosynthetic and evolution histories.

3. Classification of CEMP Stars: Shortcomings of the Current Classification Criteria and a Revised Classification Scheme for Identifying CEMP-s and CEMP-r/s Stars

Among the CEMP stars, distinguishing the CEMP-s and CEMP-r/s stars is crucial in order to understand the various astrophysical and nucleosynthetic processes responsible for the abundance patterns of the two sub-classes. The object HD 145777 in our sample, particularly posed a challenge in this regard. This object could be classified as a CEMP-r/s star based on the classification schemes of Beers and Christlieb (2005), Frebel (2018), and Hansen et al. (2019), and as a CEMP-s star if the classification criteria of Abate et al. (2016) are adopted. Based on a parametric model based analysis we have found that in order to fit the observed abundances, a model with a neutron density of $10^{10}\,\mathrm{cm}^{-3}$ is required (Goswami et al., 2021) which is towards the higher limit of the neutron density required for s-process nucleosynthesis. To remove the uncertainties and confusion regarding its classification, we have revisited the classification schemes of CEMP-s and CEMP-r/s stars found in the literature. From a detailed investigation we have seen that none of the existing classification criteria could clearly distinguish the CEMP-s and CEMP-r/s stars. We have examined if abundance ratios such as [hs/ls] (where hs implies heavy

s-process elements and ls the light s-process elements), [Sr/Ba], [Ba/Eu], [La/Eu], [La/Ce], [As/Ge] and [Se/Ge] could be used as classifiers to distinguish the CEMP-s and CEMP-r/s stars effectively. We note that the [hs/ls] peaks at different values giving higher values for CEMP-r/s stars than CEMP-s stars. However, the CEMP-s and the CEMP-r/s stars are also found to show an overlap in the range $0.0 <$ [hs/ls] < 1.5. Hence, this ratio alone cannot be used as a definitive classifier of CEMP-s and CEMP-r/s stars. Based on our investigation, we suggest that an object satisfying the criteria $0.0 <$ [Ba/Eu] < 1.0 and $0.0 <$ [La/Eu] < 0.5 can be classified as a CEMP-r/s star; however, if [La/Eu] $= 0.6 \pm 0.1$ the condition [Eu/Fe] > 1.0 also needs to be satisfied for the star to be a CEMP-r/s star. We proposed, the best criteria to distinguish the CEMP-s and CEMP-r/s stars as:

- CEMP: [C/Fe] ≥ 0.7
- CEMP-r/s: [Ba/Fe] ≥ 1.0, [Eu/Fe] ≥ 1.0
  - i) $0.0 \leq$ [Ba/Eu] ≤ 1.0 and/or $0.0 \leq$ [La/Eu] ≤ 0.7;
- CEMP-s: [Ba/Fe] ≥ 1.0
  - i.) [Eu/Fe] < 1.0, [Ba/Eu] > 0.0 and/or [La/Eu] > 0.5;
  - ii.) [Eu/Fe] ≥ 1.0, [Ba/Eu] > 1.0 and/or [La/Eu] > 0.7.

This scheme of classification based on the abundance ratios of three key neutron-capture elements barium, lanthanum and europium have proven to be highly effective in distinguishing the CEMP-s and CEMP-r/s stars. A critical investigation on the CEMP stars formation scenarios and a thorough discussion on the CEMP stars classification criteria along with the new classification scheme put forward by us are presented and discussed at length in Goswami et al. (2021).

4. Characterizing the Companion AGB Stars of CH, CEMP-s and CEMP-r/s Stars

We have investigated the mass of companion AGB stars using several diagnostics such as C, N, O, Na, Mg abundances, [hs/ls] ratio, and [Rb/Zr] ratio. The carbon isotopic ratio $^{12}C/^{13}C$ an important mixing indicator is also measured whenever possible. Na and Mg enrichment is expected to observe if the s-process over abundance is resulting from the neutrons produced during the convective thermal pulses through the reaction $^{22}Ne(\alpha,n)^{25}Mg$. Several abundance ratios of certain key elements are also used as diagnostics to understand the characteristic properties of the companion AGB stars as discussed in Shejeelammal et al. (2021); Shejeelammal and Goswami (2021, 2022); Purandardas and Goswami (2021b); Goswami et al. (2021).

4.1. The [hs/ls] ratio as an indicator of neutron source

The [hs/ls] ratio is a useful indicator of neutron source in the former companion AGB star. At higher neutron exposures, more second peak (hs) s-process elements are produced over the first peak (ls), resulting in high [hs/ls] ratio. As the neutron exposure increases with decreasing metallicity, [hs/ls] ratio increases with decreasing metallicity, showing anti-correlation with metallicity. The anti-correlation of [hs/ls] suggest the operation of ^{13}C(α, n)^{16}O neutron source, since ^{13}C(α, n)^{16}O is found to be anti-correlated with metallicity (Clayton, 1988; Wallerstein et al., 1997). Hence positive values for [hs/ls] ratio could be seen in low-mass, low metallicity AGB stars (Goriely and Mowlavi, 2000; Busso et al., 2001), whereas, in the case of massive AGB stars (5–8 $M_{\odot}$), where the neutron source is ^{22}Ne(α, n)^{25}Mg, negative values for this ratio are observed (Goriely and Siess, 2005; Karakas, 2010; Karakas et al., 2012; van Raai et al., 2012; Karakas and Lattanzio, 2014). The ^{22}Ne(α, n)^{25}Mg source has smaller neutron exposure compared to the ^{13}C(α, n)^{16}O source. Hence, in the stars where ^{22}Ne(α, n)^{25}Mg operates, we expect a lower [hs/ls] ratio. The lower neutron exposure of the neutrons produced from the ^{22}Ne source together with the predictions of low [hs/ls] ratio in massive AGB star models have been taken as the evidence of operation of ^{22}Ne(α, n)^{25}Mg in massive AGB stars. A Mg enrichment is expected in the stars where this reaction takes place. None of the CEMP stars studied by us in Shejeelammal et al. (2021); Shejeelammal and Goswami (2021, 2022) shows such an enrichment, ruling out the possibility of ^{22}Ne(α, n)^{25}Mg reaction as a possible neutron source with respect to [hs/ls] ratio. All the CEMP-r/s stars and CEMP-s stars (except HE 0920–0506 and HE 1354–2257), studied in the above mentioned studies show positive values of [hs/ls] indicating low-mass of the companion AGB stars.

4.2. Rb as a probe of neutron density at the s-process site: the [Rb/Zr] ratio

In addition to the [hs/ls] ratio, the abundance of rubidium can also provide clues to the mass of the companion AGB stars. The AGB star models predict higher Rb abundances for massive AGB stars where the neutron source is ^{22}Ne(α,n)^{25}Mg reaction (Abia et al., 2001; van Raai et al., 2012). Detailed nucleosynthesis models for the stars with masses between 5–9 $M_{\odot}$ at solar metallicity predict [Rb/(Sr,Zr)] > 0 (Karakas et al., 2012). A positive value of [Rb/Sr] or [Rb/Zr] ratio indicates a higher neutron density, whereas a negative value indicates a low neutron density with ^{13}C(α, n)^{16}O reaction acting as the neutron source. A comprehensive discussion on Rb as a probe of the mass of the companion AGB star can be found in Shejeelammal et al. (2021); Shejeelammal and Goswami (2021). In these studies the authors have found negative values for [Rb/Zr] and [Rb/Sr] ratios for stars for which these ratios could be estimated. The observed [Rb/Fe] and [Zr/Fe] ratios and the abundances of Rb and Zr are found to be consistent with the range normally observed in the low-mass AGB stars, that indicate low-mass nature of the companion AGB stars.

4.3. Determination of the mass of the companion AGB stars from a parametric model based analysis using FRUITY

Detail procedure of the parametric model based analysis to derive the mass of the companion AGB stars have been discussed at length in several of our papers (Shejeelammal and Goswami, 2021, 2022; Goswami et al., 2021; Purandardas and Goswami, 2021b; Goswami and Goswami, 2023). The mass of the AGB stars responsible for the observed abundances of the stars reported in these papers are derived by comparing the observed abundance with the predicted abundance from FRUITY models (Cristallo et al., 2009, 2011, 2015) for the heavy elements (Sr, Y, Zr, Ba, La, Ce, Pr, Nd, Sm and Eu). The best fitting mass of the companion AGB is obtained by fitting the observed abundance with the parametric model function of Husti et al. (2009) by minimizing the χ^2 value. All the stars in these studies are found to have low-mass AGB companions with $M \leq 3M_{\odot}$.

5. Origin of CEMP-r/s Stars: Clues from the Abundance Pattern and Parametric Model Based Analysis

A comprehensive discussion on the parametric model based analysis and the results obtained for the stellar sample studied by us can be found in (Goswami et al., 2021; Shejeelammal and Goswami, 2021, 2022). The overlap of [hs/ls] ratios between the CEMP-s and CEMP-r/s stars (Goswami et al., 2021) indicates that the origin of both the groups owe a common astrophysical site and process but likely under different conditions. The higher [hs/ls] ratio of the CEMP-r/s stars compared to the CEMP-s stars indicate a higher neutron exposure for their formation than the classical s-process. The tight correlation between the observed [Eu/Fe] and [hs/Fe] ratios in CEMP-r/s stars (Goswami et al., 2021) points towards a single stellar site where both the s- and r- process elements could be produced simultaneously. A higher neutron densities than that required for the classical s-process, of the order of 10^{15}–10^{17} cm^{-3}, intermediate between the s- and r-process neutron densities, could be achieved when a substantial amount of hydrogen rich-material is mixed into the intershell region of the evolved red-giant stars (Proton Ingestion Episode, PIE) undergoing helium shell flash (Cowan and Rose, 1977). There are several sites proposed to host the PIEs in order for the i-process nucleosynthesis to take place, however the astrophysical site for occurrence of i-process still remains a topic of debate.

We have used the i-process model yields [X/Fe], from Hampel et al. (2016) and compared with the observed [X/Fe] of the CEMP-r/s stars in our sample for the neutron densities ranging from 10^9 to 10^{15} cm^{-3}. We have considered only the neutron-capture elements for the comparison. The neutron-density responsible for the observed abundances in the star is derived by fitting the observed abundance with the dilution factor incorporated parametric model function:

$$\mathrm{X} = \mathrm{X}_i \cdot (1-d) + \mathrm{X}_{\odot} \cdot d$$

where X represents the final abundance, X_i the i-process abundance, d is the dilution factor and $\mathrm{X}_{\odot}$ is the solar-scaled abundance. Here d is a free parameter that can be varied to find the best fit between the model and the observational data for each constant neutron density. The best fit

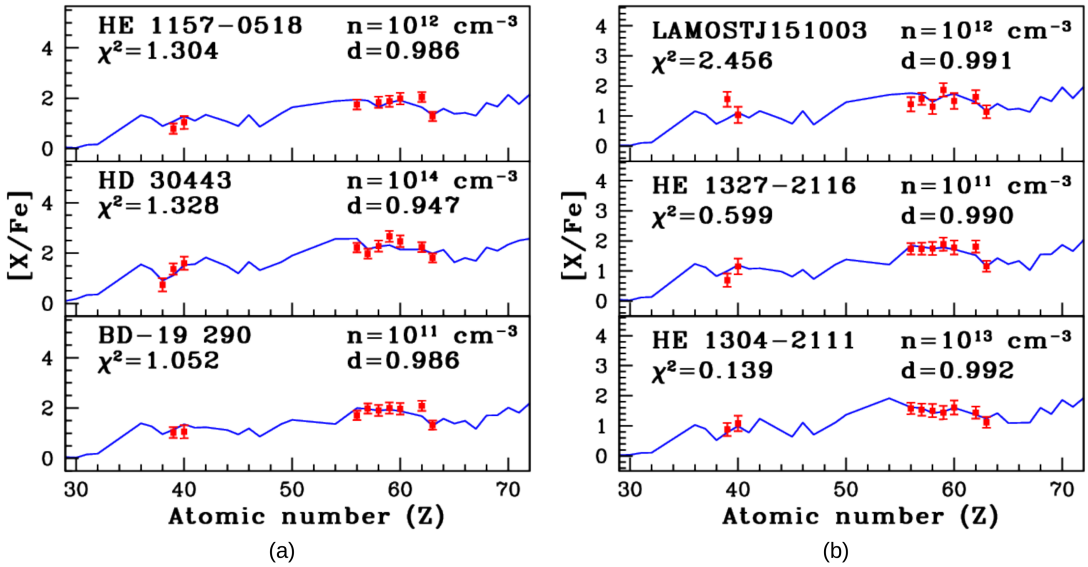

Figure 2: Parametric model fits for CEMP-r/s stars. Solid curves represent the best fit for the parametric model function. The points with error bars indicate the observed abundances.

model is found using χ^2min method. Some examples of the best fits obtained for the CEMP-r/s stars are shown in Fig. 2.

6. Observational Evidence for Multiple Origins for CEMP-no Stars

The differences in the morphology of CEMP-no stars on the Yoon–Beers diagram (A(C) - [Fe/H] diagram), leading to two distinct groups, Group II and Group III CEMP-no stars suggest multiple formation pathways for CEMP-no stars (Yoon et al., 2016). The two CEMP-no stars HE 2148–2039 and HE 2155–2043 studied by us (Purandardas and Goswami, 2021a) are also found to provide observational evidence for multiple origins for CEMP-no stars. These two objects are found to have similar metallicity ([Fe/H] of -3.32 and -3.46, respectively) and enhanced carbon with [C/Fe] values of 1.27 and 2.05, respectively. While Mg is found to be under abundant in HE 2148–2039 with [Mg/Fe] $= -0.35$, it is highly enhanced in HE 2155–2043 with [Mg/Fe] $= 1.57$, indicating different origins as far as the α-elements are concerned. As far as the heavy elements are concerned, while HE 2148–2039 shows a very strong feature of Ba II 4934.06 Å and a weak feature of Sr II 4215.52 Å; in contrast, the object HE 2155–2043 shows a strong feature of Sr II 4215.52 Å and a weak feature of Ba II 4934.06 Å (Fig. 3). The estimated [Sr/Fe] and [Ba/Fe] are -2.02 and -0.84, resp., for HE 2148–2039 and -0.04, resp., -1.64 for HE 2155–2043. These differences clearly indicate different origins for these two objects. The locations of these two stars in the absolute carbon abundance, A(C) versus [Fe/H] diagram, show that HE 2148–2039 is a CEMP-no Group II object and HE 2155–2043 is a CEMP-no Group III object (Purandardas and Goswami, 2021a).

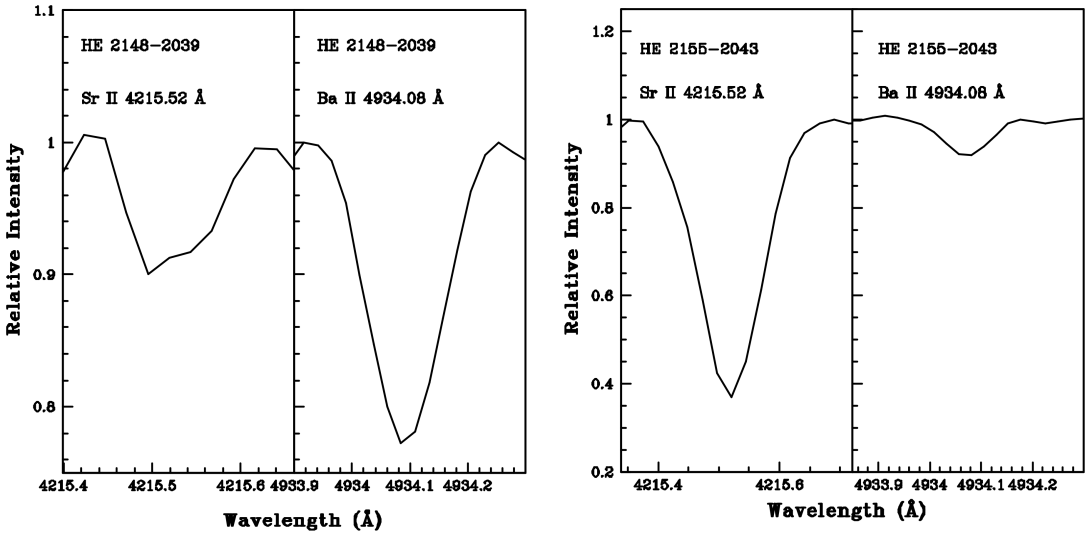

(a) (b)

Figure 3: While Ba II 4934.08 Å is marginally detectable in HE 2155–2043, this feature appears strong in HE 2048–2039. On the other hand, Sr II 4215.52 Å feature is strong in HE 2155–2043 and weak in HE 2148–2039. Both the objects are of similar metallicity [Fe/H] $<$ -3.3 and [C/Fe] > 1.0.

7. HE 1005–1439: A Unique Star with Dual Nucleosynthesis Dignatures

This object with a unique abundance pattern that shows dual nucleosynthesis signatures was first reported in Goswami and Goswami (2022). The star was found to be extremely metal-poor with [Fe/H] $= -3.03$ and heavily enriched with neutron-capture elements. The observed elemental abundances of the object could not be explained based on theoretical s-, r-, or i-process model predictions alone. We have performed a parametric-model-based analysis of the abundances of the heavy elements which indicated that the star's surface chemical composition is being influenced by similar contributions from both the s- and i-processes. This forms a new class of object of distinct abundance pattern with dual nucleosynthesis signatures.

The estimated radial velocities of the object from several epochs showed variations indicating the presence of a binary companion. Based on this observation, we proposed a formation scenario for HE 1005–1439 involving mass transfer from a now extinct AGB companion where both i- and s-process nucleosynthesis took place during various stages of the AGB evolution with proton ingestion episodes (PIEs) triggering i-process followed by s-process AGB nucleosynthesis with a few third-dredge-up episodes. A detailed study on this object and the significance of the results obtained are presented in Goswami and Goswami (2022).

8. A Few Critical Issues in the Analysis of CEMP Stars

To understand the role of CEMP stars on Galactic chemical evolution, accurate knowledge of the CEMP fractions among the metal-poor stars of the Galactic halo is vital. The fraction is found to have different values based on the adopted definition of CEMP stars, i.e., either

[C/Fe] > 1.0 (Beers and Christlieb, 2005), or [C/Fe] ≥ 0.7 (Aoki et al., 2007). A compilation of published CEMP fractions and samples of Galactic halo stars from the past 25 years, revealed that they are not all consistent with each other (Arentsen et al., 2022). Significant differences were noticed between various surveys when comparing their trends of [Fe/H] versus [C/Fe] and their distributions of CEMP stars. These discrepancies were primarily attributed to the differences in the analysis procedures and criteria adopted by different groups.

The application of the empirical correction to the [C/Fe] values based on the evolutionary stage of a star and its metallicity is essential for a homogeneous analysis and interpretation. Hence, in order to have accurate carbon estimates the necessary evolutionary correction to the observed carbon abundance values needs to be applied.

Most of the known CEMP stars are giants or sub-giants. The stars on the red-giant branch (RGB) undergo internal mixing and hence alters the surface CN abundances (e.g., Aoki et al., 2007; Gratton et al., 2000; Placco et al., 2014). Placco et al. (2014) derived [C/Fe] corrections based on evolutionary stage of a star and its metallicity. The application of the empirical correction to the [C/Fe] values from Aguado et al. (2019) resulted in reducing the total number of CEMP stars from 64 to 12 (Arentsen et al., 2022). Based on the analysis of a sample of 505 metal-poor ([Fe/H] ≤ -2) stars with no enhancement of neutron-capture elements from the literature, Placco et al. (2014) have shown that the frequency of CEMP-no stars ([C/Fe] ≥ 0.7) in the Galaxy is increased by $\sim 11\%$ for [Fe/H] ≤ -3 when proper correction required for the carbon depletion is applied to the observed [C/Fe]. A comparison of the [C/Fe] ratios obtained using corrected and non-corrected carbon abundance as a function of $\log g$ is shown in Fig. 4 for CEMP stars from the literature (Placco et al., 2014) and references therein) and our program stars.

Since CEMP-s and CEMP-no stars have very different progenitors, their relative fraction provide insight into the different physical processes at different metallicity. Hence, identification of genuine CEMP-no stars and CEMP-s and accurate knowledge of CEMP-s and CEMP-no fractions among CEMP stars is crucial.

The G-band of CH is commonly used as carbon abundance diagnostics in CEMP stars. Most of these estimates are based on LTE assumption. In a recent study, Popa et al. (2023) have explored the sensitivity of this feature to NLTE effects considering the case of the Sun and red-giant stars. They found that in the statistical equilibrium of the CH molecule this effect is significant, increases with decreasing metallicity, and cannot be neglected for precision spectroscopic analysis of C abundances. The C abundance is under-estimated if LTE is assumed. The non-LTE corrections to C abundance inferred from the CH band range from $+0.04$ dex to 0.2 dex for a red giant with metallicity [Fe/H] $= -4.0$.

Sample selection is also crucial while determining CEMP fractions. Only stars of similar evolutionary phases should be used to compare CEMP samples to ensure similar evolutionary paths, similar systematic errors and to minimize biases.

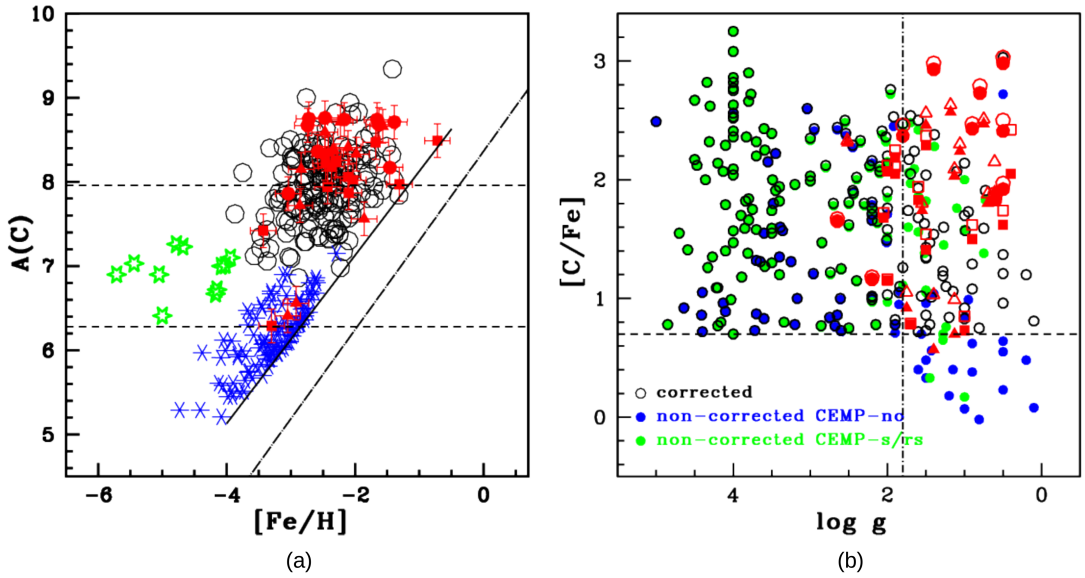

Figure 4: (a) Absolute carbon abundance A(C) with respect to metallicity [Fe/H] are plotted for CEMP stars. Black circles represent Group I CEMP-s and CEMP-r/s stars, blue crosses Group II CEMP-no stars, and the green stars represent the Group III CEMP-no stars from the literature (Yoon et al. (2016) and references therein). Red triangles represent CEMP stars from Shejeelammal et al. (2021), Shejeelammal and Goswami (2021, 2022) and Shejeelammal and Goswami (2023, in prep.). Red rectangles represent CEMP stars from Purandardas et al. (2019) and Purandardas and Goswami (2021a,b) The red circles represent CEMP stars from Goswami et al. (2021) and Goswami and Goswami (2022, 2023) The black dashed lines indicate - high and low carbon bands at A(C) $\sim$ 7.96 and 6.28. The solid line corresponds to [C/Fe] = 0.70 and the long-dash dot line corresponds to [C/Fe] = 0. (b) [C/Fe] ratio as a function of $\log g$ for CEMP stars from the literature (Placco et al. (2014) and references therein). The observed [C/Fe] for CEMP-no stars are represented by blue filled circles, the CEMP-s and CEMP-r/s stars by green filled circles, and the corrected [C/Fe] by black open circles. Red triangles indicate CEMP stars from Shejeelammal et al. (2021), Shejeelammal and Goswami (2021, 2022) and Shejeelammal and Goswami (2023, in prep.). Red rectangles represent CEMP stars from Purandardas et al. (2019) and Purandardas and Goswami (2021a,b) Red circles represent CEMP stars from Goswami et al. (2021) and Goswami and Goswami (2022, 2023). The filled symbols are used for observed values and the open symbols are used for the corrected values. The dashed horizontal line corresponds to [C/Fe] = 0.7, and the vertical dot-dashed line corresponds to $\log g = 1.8$.

9. Concluding Remarks

Some highlights of the results obtained from low- and high-resolution spectroscopic analysis of CEMP stars are presented. A new classification scheme put forward by Goswami et al. (2021) clearly distinguishes CEMP-s and CEMP-r/s stars. Detailed abundance analysis of CH, CEMP-s and CEMP-r/s stars re-confirms pollution from low-mass AGB companion. Parametric model based analysis performed for CH, CEMP-s and CEMP-r/s stars also confirm low-mass for their former companion AGB stars. Our analysis confirms that a modified s-process the so-called i-process, is responsible for the observed abundance pattern in CEMP-r/s stars. The i-process models could successfully reproduce the observed abundance in CEMP-r/s stars.

Peculiar abundances of HE 1005–1439 present first ever observational evidence of the occurrence of dual nucleosynthesis in the companion AGB star, the i-process followed by s-process in various stages of the AGB evolution, with PIEs triggering i-process followed by s-process during third-dredge-up episodes.

Surface chemical composition and spectral signatures of two extremely metal-poor CEMP-no stars HE 2148–2039 and HE 2155–2043 reaffirm multiple origins for CEMP-no stars.

Knowing the fraction of CEMP stars relative to carbon-normal stars is important for interpretation of populations of metal-poor stars. However, classification and hence the fraction of each class is not possible to estimate accurately based on low-resolution spectroscopy.

The fraction of CEMP stars as a function of metallicity, how it changes with the different classes of CEMP stars and different stellar evolutionary phases are some of the outstanding questions that are yet to find clear answers. More homogeneous analysis of larger samples are needed to unravel the full potential of CEMP stars for Galactic Archaeology.

Acknowledgments

AG acknowledges the support received from the Belgo-Indian Network for Astronomy & Astrophysics project BINA–2 (DST/INT/Belg/P-02 (India) and BL/11/IN07 (Belgium)).

Further Information

Authors' ORCID identifiers

0000-0002-8841-8641 (Aruna GOSWAMI)
0000-0002-6234-4226 (Jameela SHEJEELAMMAL)
0000-0002-5081-3208 (Partha Pratim GOSWAMI)
0000-0001-5047-5950 (Meenakshi PURANDARDAS)

Author contributions

This work is part of a collective effort with contributions from all the co-authors.

Conflicts of interest

The authors declare no conflict of interest.

References

Abate, C., Stancliffe, R. J. and Liu, Z.-W. (2016) How plausible are the proposed formation scenarios of CEMP-r/s stars? A&A, 587, A50. https://doi.org/10.1051/0004-6361/201527864.

Abia, C., Busso, M., Gallino, R., Domínguez, I., Straniero, O. and Isern, J. (2001) The ^{85}Kr s-process branching and the mass of carbon stars. ApJ, 559(2), 1117–1134. https://doi.org/10.1086/322383.

Aguado, D. S., Youakim, K., González Hernández, J. I., Allende Prieto, C., Starkenburg, E., Martin, N., Bonifacio, P., Arentsen, A., Caffau, E., Peralta de Arriba, L., Sestito, F., Garcia-Dias, R., Fantin, N., Hill, V., Jablonca, P., Jahandar, F., Kielty, C., Longeard, N., Lucchesi, R., Sánchez-Janssen, R., Osorio, Y., Palicio, P. A., Tolstoy, E., Wilson, T. G., Côté, P., Kordopatis, G., Lardo, C., Navarro, J. F., Thomas, G. F. and Venn, K. (2019) The Pristine survey – VI. The first three years of medium-resolution follow-up spectroscopy of Pristine EMP star candidates. MNRAS, 490(2), 2241–2253. https://doi.org/10.1093/mnras/stz2643.

Aoki, W., Beers, T. C., Christlieb, N., Norris, J. E., Ryan, S. G. and Tsangarides, S. (2007) Carbon-enhanced metal-poor stars. I. Chemical compositions of 26 stars. ApJ, 655, 492–521. https://doi.org/10.1086/509817.

Aoki, W., Beers, T. C., Lee, Y. S., Honda, S., Ito, H., Takada-Hidai, M., Frebel, A., Suda, T., Fujimoto, M. Y., Carollo, D. and Sivarani, T. (2013) High-resolution spectroscopy of extremely metal-poor stars from SDSS/SEGUE. I. Atmospheric parameters and chemical compositions. AJ, 145(1), 13. https://doi.org/10.1088/0004-6256/145/1/13.

Arentsen, A., Placco, V. M., Lee, Y. S., Aguado, D. S., Martin, N. F., Starkenburg, E. and Yoon, J. (2022) On the inconsistency of [C/Fe] abundances and the fractions of carbon-enhanced metal-poor stars among various stellar surveys. MNRAS, 515(3), 4082–4098. https://doi.org/10.1093/mnras/stac2062.

Arentsen, A., Starkenburg, E., Shetrone, M. D., Venn, K. A., Depagne, É. and McConnachie, A. W. (2019) Binarity among CEMP-no stars: an indication of multiple formation pathways? A&A, 621, A108. https://doi.org/10.1051/0004-6361/201834146.

Beers, T. C. (1999) Low-metallicity and horizontal-branch stars in the halo of the Galaxy. ASPC, 165, 202.

Beers, T. C. and Christlieb, N. (2005) The discovery and analysis of very metal-poor stars in the Galaxy. ARAA, 43(1), 531–580. https://doi.org/10.1146/annurev.astro.42.053102.134057.

Beers, T. C., Flynn, C., Rossi, S., Sommer-Larsen, J., Wilhelm, R., Marsteller, B., Lee, Y. S., De Lee, N., Krugler, J., Deliyannis, C. P., Simmons, A. T., Mills, E., Zickgraf, F.-J., Holmberg, J., Önehag, A., Eriksson, A., Terndrup, D. M., Salim, S., Andersen, J., Nordström, B., Christlieb, N., Frebel, A. and Rhee, J. (2007) Broadband $UBVR_{\rm C}I_{\rm C}$ photometry of horizontal-branch and metal-poor candidates from the HK and Hamburg/ESO surveys. I. ApJS, 168(1), 128–139. https://doi.org/10.1086/509324.

Beers, T. C., Preston, G. W. and Shectman, S. A. (1985) A search for stars of very low metal abundance. I. AJ, 90, 2089–2102. https://doi.org/10.1086/113917.

Beers, T. C., Preston, G. W. and Shectman, S. A. (1992) A search for stars of very low metal abundance. II. AJ, 103, 1987. https://doi.org/10.1086/116207.

Bisterzo, S., Gallino, R., Straniero, O., Cristallo, S. and Käppeler, F. (2011) The s-process in low-metallicity stars – II. Interpretation of high-resolution spectroscopic observations with asymptotic giant branch models. MNRAS, 418(1), 284–319. https://doi.org/10.1111/j.1365-2966.2011.19484.x.

Bonifacio, P., Caffau, E., Spite, M., Limongi, M., Chieffi, A., Klessen, R. S., François, P., Molaro, P., Ludwig, H. G., Zaggia, S., Spite, F., Plez, B., Cayrel, R., Christlieb, N., Clark, P. C., Glover, S. C. O., Hammer, F., Koch, A., Monaco, L., Sbordone, L. and Steffen, M. (2015) TOPoS. II. On the bimodality of carbon abundance in cemp stars Implications on the early chemical evolution of galaxies. A&A, 579, A28. https://doi.org/10.1051/0004-6361/201425266.

Busso, M., Gallino, R., Lambert, D. L., Travaglio, C. and Smith, V. V. (2001) Nucleosynthesis and mixing on the asymptotic giant branch. III. Predicted and observed *s*-process abundances. ApJ, 557(2), 802–821. https://doi.org/10.1086/322258.

Busso, M., Gallino, R. and Wasserburg, G. J. (1999) Nucleosynthesis in asymptotic giant branch stars: Relevance for galactic enrichment and solar system formation. ARAA, 37, 239–309. https://doi.org/10.1146/annurev.astro.37.1.239.

Campbell, S. W. and Lattanzio, J. C. (2008) Evolution and nucleosynthesis of extremely metal-poor and metal-free low- and intermediate-mass stars. I. Stellar yield tables and the CEMPs. A&A, 490(2), 769–776. https://doi.org/10.1051/0004-6361:200809597.

Campbell, S. W., Lugaro, M. and Karakas, A. I. (2010) Evolution and nucleosynthesis of extremely metal-poor and metal-free low- and intermediate-mass stars. II. *s*-process nucleosynthesis during the core He flash. A&A, 522, L6. https://doi.org/10.1051/0004-6361/201015428.

Carollo, D., Beers, T. C., Bovy, J., Sivarani, T., Norris, J. E., Freeman, K. C., Aoki, W., Lee, Y. S. and Kennedy, C. R. (2012) Carbon-enhanced metal-poor stars in the inner and outer halo components of the Milky Way. ApJ, 744(2), 195. https://doi.org/10.1088/0004-637X/744/2/195.

Carollo, D., Beers, T. C., Lee, Y. S., Chiba, M., Norris, J. E., Wilhelm, R., Sivarani, T., Marsteller, B., Munn, J. A., Bailer-Jones, C. A. L., Fiorentin, P. R. and York, D. G. (2007) Two stellar components in the halo of the Milky Way. Natur, 450(7172), 1020–1025. https://doi.org/10.1038/nature06460.

Choplin, A., Hirschi, R., Meynet, G. and Ekström, S. (2017) Are some CEMP-s stars the daughters of spinstars? A&A, 607, L3. https://doi.org/10.1051/0004-6361/201731948.

Christlieb, N. (2003) Finding the most metal-poor stars of the Galactic halo with the Hamburg/ESO objective-prism survey. RvMA, 16, 191. https://doi.org/10.1002/9783527617647.ch8.

Christlieb, N., Green, P. J., Wisotzki, L. and Reimers, D. (2001a) The stellar content of the Hamburg/ESO survey. II. A large, homogeneously-selected sample of high latitude carbon stars. A&A, 375, 366–374. https://doi.org/10.1051/0004-6361:20010814.

Christlieb, N., Schörck, T., Frebel, A., Beers, T. C., Wisotzki, L. and Reimers, D. (2008) The stellar content of the Hamburg/ESO survey. IV. Selection of candidate metal-poor stars. A&A, 484(3), 721–732. https://doi.org/10.1051/0004-6361:20078748.

Christlieb, N., Wisotzki, L., Reimers, D., Homeier, D., Koester, D. and Heber, U. (2001b) The stellar content of the Hamburg/ESO survey. I. Automated selection of DA white dwarfs. A&A, 366, 898–912. https://doi.org/10.1051/0004-6361:20000269.

Clarkson, O., Herwig, F. and Pignatari, M. (2018) Pop III *i*-process nucleosynthesis and the elemental abundances of SMSS J0313-6708 and the most iron-poor stars. MNRAS, 474(1), L37–L41. https://doi.org/10.1093/mnrasl/slx190.

Clayton, D. D. (1988) Nuclear cosmochronology within analytic models of the chemical evolution of the solar neighbourhood. MNRAS, 234, 1–36. https://doi.org/10.1093/mnras/234.1.1.

Cowan, J. J. and Rose, W. K. (1977) Production of ^{14}C and neutrons in red giants. ApJ, 212, 149–158. https://doi.org/10.1086/155030.

Cristallo, S., Karinkuzhi, D., Goswami, A., Piersanti, L. and Gobrecht, D. (2016) Constraints of the physics of low-mass AGB stars from CH and CEMP stars. ApJ, 833(2), 181. https://doi.org/10.3847/1538-4357/833/2/181.

Cristallo, S., Piersanti, L., Straniero, O., Gallino, R., Domínguez, I., Abia, C., Di Rico, G., Quintini, M. and Bisterzo, S. (2011) Evolution, nucleosynthesis, and yields of low-mass asymptotic giant branch stars at different metallicities. II. The FRUITY database. ApJS, 197(2), 17. https://doi.org/10.1088/0067-0049/197/2/17.

Cristallo, S., Straniero, O., Gallino, R., Piersanti, L., Domínguez, I. and Lederer, M. T. (2009) Evolution, nucleosynthesis, and yields of low-mass asymptotic giant branch stars at different metallicities. ApJ, 696(1), 797–820. https://doi.org/10.1088/0004-637X/696/1/797.

Cristallo, S., Straniero, O., Piersanti, L. and Gobrecht, D. (2015) Evolution, nucleosynthesis, and yields of agb stars at different metallicities. III. Intermediate–mass models, revised low-mass models, and the ph-FRUITY interface. ApJS, 219(2), 40. https://doi.org/10.1088/0067-0049/219/2/40.

Cruz, M. A., Serenelli, A. and Weiss, A. (2013) S-process in extremely metal-poor, low-mass stars. A&A, 559, A4. https://doi.org/10.1051/0004-6361/201219513.

Cui, X.-Q., Zhao, Y.-H., Chu, Y.-Q., Li, G.-P., Li, Q., Zhang, L.-P., Su, H.-J., Yao, Z.-Q., Wang, Y.-N., Xing, X.-Z., Li, X.-N., Zhu, Y.-T., Wang, G., Gu, B.-Z., Luo, A. L., Xu, X.-Q., Zhang, Z.-C., Liu, G.-R., Zhang, H.-T., Yang, D.-H., Cao, S.-Y., Chen, H.-Y., Chen, J.-J., Chen, K.-X., Chen, Y., Chu, J.-R., Feng, L., Gong, X.-F., Hou, Y.-H., Hu, H.-Z., Hu, N.-S., Hu, Z.-W., Jia, L., Jiang, F.-H., Jiang, X., Jiang, Z.-B., Jin, G., Li, A.-H., Li, Y., Li, Y.-P., Liu, G.-Q., Liu, Z.-G., Lu, W.-Z., Mao, Y.-D., Men, L., Qi, Y.-J., Qi, Z.-X., Shi, H.-M., Tang, Z.-H., Tao, Q.-S., Wang, D.-Q., Wang, D., Wang, G.-M., Wang, H., Wang, J.-N., Wang, J., Wang, J.-L., Wang, J.-P., Wang, L., Wang, S.-Q., Wang, Y., Wang, Y.-F., Xu, L.-Z., Xu, Y., Yang, S.-H., Yu, Y., Yuan, H., Yuan, X.-Y., Zhai, C., Zhang, J., Zhang, Y.-X., Zhang, Y., Zhao, M., Zhou, F., Zhou, G.-H., Zhu, J. and Zou, S.-C. (2012) The Large Sky Area Multi-Object fiber Spectroscopic Telescope (LAMOST). RAA, 12(9), 1197–1242. https://doi.org/10.1088/1674-4527/12/9/003.

de Bennassuti, M., Salvadori, S., Schneider, R., Valiante, R. and Omukai, K. (2017) Limits on Population III star formation with the most iron-poor stars. MNRAS, 465(1), 926–940. https://doi.org/10.1093/mnras/stw2687.

Deng, L.-C., Newberg, H. J., Liu, C., Carlin, J. L., Beers, T. C., Chen, L., Chen, Y.-Q., Christlieb, N., Grillmair, C. J., Guhathakurta, P., Han, Z.-W., Hou, J.-L., Lee, H.-T., Lépine, S., Li, J., Liu, X.-W., Pan, K.-K., Sellwood, J. A., Wang, B., Wang, H.-C., Yang, F., Yanny, B., Zhang, H.-T., Zhang, Y.-Y., Zheng, Z. and Zhu, Z. (2012) LAMOST Experiment for Galactic Understanding and Exploration (LEGUE) — The survey's science plan. RAA, 12(7), 735–754. https://doi.org/10.1088/1674-4527/12/7/003.

Denissenkov, P. A., Herwig, F., Battino, U., Ritter, C., Pignatari, M., Jones, S. and Paxton, B. (2017) I-process nucleosynthesis and mass retention efficiency in He-shell flash evolution of rapidly accreting white dwarfs. ApJ, 834(2), L10. https://doi.org/10.3847/2041-8213/834/2/L10.

Doherty, C. L., Gil-Pons, P., Siess, L., Lattanzio, J. C. and Lau, H. H. B. (2015) Super– and massive AGB stars – IV. Final fates – initial-to-final mass relation. MNRAS, 446(3), 2599–2612. https://doi.org/10.1093/mnras/stu2180.

Frebel, A. (2018) From nuclei to the cosmos: Tracing heavy-element production with the oldest stars. ARNPS, 68(1), 237–269. https://doi.org/10.1146/annurev-nucl-101917-021141.

Frebel, A. and Ji, A. P. (2023) Observations of r-process stars in the Milky Way and dwarf galaxies. arXiv:2302.09188. https://doi.org/10.48550/arXiv.2302.09188.

Frebel, A. and Norris, J. E. (2015) Near-field cosmology with extremely metal-poor stars. ARAA, 53, 631–688. https://doi.org/10.1146/annurev-astro-082214-122423.

Frischknecht, U., Hirschi, R. and Thielemann, F. K. (2012) Non-standard s-process in low metallicity massive rotating stars. A&A, 538, L2. https://doi.org/10.1051/0004-6361/201117794.

Gil-Pons, P., Doherty, C. L., Gutiérrez, J., Campbell, S. W., Siess, L. and Lattanzio, J. C. (2021) Nucleosynthetic yields of $Z = 10^{-5}$ intermediate-mass stars. A&A, 645, A10. https://doi.org/10.1051/0004-6361/201937264.

Goriely, S. and Mowlavi, N. (2000) Neutron-capture nucleosynthesis in AGB stars. A&A, 362, 599–614.

Goriely, S. and Siess, L. (2005) The s-process nucleosynthesis. IAUS, 228, 451–460. https://doi.org/10.1017/S1743921305006204.

Goswami, A. (2005) CH stars at high Galactic latitudes. MNRAS, 359, 531–544. https://doi.org/10.1111/j.1365-2966.2005.08917.x.

Goswami, A., Karinkuzhi, D. and Shantikumar, N. S. (2010) The CH fraction of carbon stars at high Galactic latitudes. MNRAS, 402(2), 1111–1125. https://doi.org/10.1111/j.1365-2966.2009.15939.x.

Goswami, P. P. and Goswami, A. (2022) The peculiar abundances of HE 1005–1439. A carbon-enhanced extremely metal-poor star contaminated with products of both *s*- and *i*-process nucleosynthesis. A&A, 657, A50. https://doi.org/10.1051/0004-6361/202141775.

Goswami, P. P. and Goswami, A. (2023) Spectroscopic study of Ba and CEMP-*s* stars: Mass distribution of AGB progenitors. AJ, 165(4), 154. https://doi.org/10.3847/1538-3881/aca971.

Goswami, P. P., Rathour, R. S. and Goswami, A. (2021) Spectroscopic study of CEMP-(s & r/s) stars. Revisiting classification criteria and formation scenarios, highlighting *i*-process nucleosynthesis. A&A, 649, A49. https://doi.org/10.1051/0004-6361/202038258.

Gratton, R. G., Sneden, C., Carretta, E. and Bragaglia, A. (2000) Mixing along the red giant branch in metal-poor field stars. A&A, 354, 169–187.

Hampel, M., Karakas, A. I., Stancliffe, R. J., Meyer, B. S. and Lugaro, M. (2019) Learning about the intermediate neutron-capture process from lead abundances. ApJ, 887(1), 11. https://doi.org/10.3847/1538-4357/ab4fe8.

Hampel, M., Stancliffe, R. J., Lugaro, M. and Meyer, B. S. (2016) The intermediate neutron-capture process and carbon-enhanced metal-poor stars. ApJ, 831(2), 171. https://doi.org/10.3847/0004-637X/831/2/171.

Hansen, C. J., Hansen, T. T., Koch, A., Beers, T. C., Nordström, B., Placco, V. M. and Andersen, J. (2019) Abundances and kinematics of carbon-enhanced metal-poor stars in the Galactic halo. A new classification scheme based on Sr and Ba. A&A, 623, A128. https://doi.org/10.1051/0004-6361/201834601.

Hansen, C. J., Nordström, B., Bonifacio, P., Spite, M., Andersen, J., Beers, T. C., Cayrel, R., Spite, F., Molaro, P., Barbuy, B., Depagne, E., François, P., Hill, V., Plez, B. and Sivarani, T. (2011) First stars. XIII. Two extremely metal-poor RR Lyrae stars. A&A, 527, A65. https://doi.org/10.1051/0004-6361/201015076.

Hansen, T., Hansen, C. J., Christlieb, N., Beers, T. C., Yong, D., Bessell, M. S., Frebel, A., García Pérez, A. E., Placco, V. M., Norris, J. E. and Asplund, M. (2015) An elemental assay of very, extremely, and ultra-metal-poor stars. ApJ, 807(2), 173. https://doi.org/10.1088/0004-637X/807/2/173.

Hansen, T. T., Andersen, J., Nordström, B., Beers, T. C., Placco, V. M., Yoon, J. and Buchhave, L. A. (2016) The role of binaries in the enrichment of the early galactic halo. II. Carbon-enhanced metal-poor stars: CEMP-no stars. A&A, 586, A160. https://doi.org/10.1051/0004-6361/201527235.

Hartwig, T., Bromm, V., Klessen, R. S. and Glover, S. C. O. (2015) Constraining the primordial initial mass function with stellar archaeology. MNRAS, 447(4), 3892–3908. https://doi.org/10.1093/mnras/stu2740.

Herwig, F., Pignatari, M., Woodward, P. R., Porter, D. H., Rockefeller, G., Fryer, C. L., Bennett, M. and Hirschi, R. (2011) Convective-reactive proton–^{12}C combustion in Sakurai's object (V4334 Sagittarii) and implications for the evolution and yields from the first generations of stars. ApJ, 727(2), 89. https://doi.org/10.1088/0004-637X/727/2/89.

Herwig, F., Woodward, P. R., Lin, P.-H., Knox, M. and Fryer, C. (2014) Global non-spherical oscillations in three-dimensional 4π simulations of the H-ingestion flash. ApJ, 792(1), L3. https://doi.org/10.1088/2041-8205/792/1/L3.

Hollek, J. K., Frebel, A., Placco, V. M., Karakas, A. I., Shetrone, M., Sneden, C. and Christlieb, N. (2015) The chemical abundances of stars in the halo (CASH) project. III. A new classification scheme for carbon-enhanced metal–poor stars with s-process element enhancement. ApJ, 814(2), 121. https://doi.org/10.1088/0004-637X/814/2/121.

Husti, L., Gallino, R., Bisterzo, S., Straniero, O. and Cristallo, S. (2009) Barium stars: Theoretical interpretation. PASA, 26(3), 176–183. https://doi.org/10.1071/AS08065.

Jones, S., Ritter, C., Herwig, F., Fryer, C., Pignatari, M., Bertolli, M. G. and Paxton, B. (2016) H ingestion into He-burning convection zones in super-AGB stellar models as a potential site for intermediate neutron-density nucleosynthesis. MNRAS, 455(4), 3848–3863. https://doi.org/10.1093/mnras/stv2488.

Jonsell, K., Barklem, P. S., Gustafsson, B., Christlieb, N., Hill, V., Beers, T. C. and Holmberg, J. (2006) The Hamburg/ESO R-process enhanced star survey (HERES). III. HE 0338–3945 and the formation of the $r+s$ stars. A&A, 451, 651–670. https://doi.org/10.1051/0004-6361:20054470.

Jorissen, A., Van Eck, S., Van Winckel, H., Merle, T., Boffin, H. M. J., Andersen, J., Nordström, B., Udry, S., Masseron, T., Lenaerts, L. and Waelkens, C. (2016) Binary properties of CH and carbon-enhanced metal-poor stars. A&A, 586, A158. https://doi.org/10.1051/0004-6361/201526992.

Karakas, A. I. (2010) Updated stellar yields from asymptotic giant branch models. MNRAS, 403(3), 1413–1425. https://doi.org/10.1111/j.1365-2966.2009.16198.x.

Karakas, A. I., García-Hernández, D. A. and Lugaro, M. (2012) Heavy element nucleosynthesis in the brightest galactic asymptotic giant branch stars. ApJ, 751(1), 8. https://doi.org/10.1088/0004-637X/751/1/8.

Karakas, A. I. and Lattanzio, J. C. (2014) The Dawes Review 2: Nucleosynthesis and stellar yields of low- and intermediate-mass single stars. PASA, 31, e030. https://doi.org/10.1017/pasa.2014.21.

Karinkuzhi, D. and Goswami, A. (2014) Chemical analysis of CH stars – I. Atmospheric parameters and elemental abundances. MNRAS, 440(2), 1095–1113. https://doi.org/10.1093/mnras/stu148.

Karinkuzhi, D. and Goswami, A. (2015) Chemical analysis of CH stars – II. Atmospheric parameters and elemental abundances. MNRAS, 446(3), 2348–2362. https://doi.org/10.1093/mnras/stu2079.

Keenan, P. C. (1942) The spectra of CH stars. ApJ, 96, 101. https://doi.org/10.1086/144435.

Klessen, R. S., Glover, S. C. O. and Clark, P. C. (2012) On the formation of very metal poor stars: the case of SDSS J1029151+172927. MNRAS, 421(4), 3217–3221. https://doi.org/10.1111/j.1365-2966.2012.20544.x.

Koch, A., Reichert, M., Hansen, C. J., Hampel, M., Stancliffe, R. J., Karakas, A. and Arcones, A. (2019) Unusual neutron-capture nucleosynthesis in a carbon-rich galactic bulge star. A&A, 622, A159. https://doi.org/10.1051/0004-6361/201834241.

Lee, Y. S., Beers, T. C., Masseron, T., Plez, B., Rockosi, C. M., Sobeck, J., Yanny, B., Lucatello, S., Sivarani, T., Placco, V. M. and Carollo, D. (2013) Carbon-enhanced metal-poor stars in SDSS/SEGUE. I. Carbon abundance estimation and frequency of CEMP stars. AJ, 146(5), 132. https://doi.org/10.1088/0004-6256/146/5/132.

Lucatello, S., Beers, T. C., Christlieb, N., Barklem, P. S., Rossi, S., Marsteller, B., Sivarani, T. and Lee, Y. S. (2006) The frequency of carbon-enhanced metal-poor stars in the Galaxy from the HERES sample. ApJ, 652(1), L37–L40. https://doi.org/10.1086/509780.

Lucatello, S., Tsangarides, S., Beers, T. C., Carretta, E., Gratton, R. G. and Ryan, S. G. (2005) The binary frequency among carbon-enhanced, *s*-process-rich, metal-poor stars. ApJ, 625(2), 825–832. https://doi.org/10.1086/428104.

Maeder, A. and Meynet, G. (2015) The first stars: a classification of CEMP-no stars. A&A, 580, A32. https://doi.org/10.1051/0004-6361/201526234.

Maeder, A., Meynet, G. and Chiappini, C. (2015) The first stars: CEMP-no stars and signatures of spinstars. A&A, 576, A56. https://doi.org/10.1051/0004-6361/201424153.

Masseron, T., Johnson, J. A., Plez, B., van Eck, S., Primas, F., Goriely, S. and Jorissen, A. (2010) A holistic approach to carbon-enhanced metal-poor stars. A&A, 509, A93. https://doi.org/10.1051/0004-6361/200911744.

McClure, R. D. and Woodsworth, A. W. (1990) The binary nature of the barium and CH stars. III. Orbital parameters. ApJ, 352, 709. https://doi.org/10.1086/168573.

Meynet, G., Ekström, S. and Maeder, A. (2006) The early star generations: the dominant effect of rotation on the CNO yields. A&A, 447(2), 623–639. https://doi.org/10.1051/0004-6361:20053070.

Norris, J. E., Gilmore, G., Wyse, R. F. G., Yong, D. and Frebel, A. (2010) An extremely carbon-rich, extremely metal-poor star in the Segue 1 system. ApJ, 722(1), L104–L109. https://doi.org/10.1088/2041-8205/722/1/L104.

Norris, J. E. and Yong, D. (2019) The most metal-poor stars. V. The CEMP-no stars in 3D and non-LTE. ApJ, 879(1), 37. https://doi.org/10.3847/1538-4357/ab1f84.

Placco, V. M., Frebel, A., Beers, T. C., Karakas, A. I., Kennedy, C. R., Rossi, S., Christlieb, N. and Stancliffe, R. J. (2013) Metal-poor stars observed with the Magellan Telescope. I. Constraints on progenitor mass and metallicity of AGB stars undergoing *s*-process nucleosynthesis. ApJ, 770(2), 104. https://doi.org/10.1088/0004-637X/770/2/104.

Placco, V. M., Frebel, A., Beers, T. C. and Stancliffe, R. J. (2014) Carbon-enhanced metal-poor star frequencies in the Galaxy: Corrections for the effect of evolutionary status on carbon abundances. ApJ, 797(1), 21. https://doi.org/10.1088/0004-637X/797/1/21.

Popa, S. A., Hoppe, R., Bergemann, M., Hansen, C. J., Plez, B. and Beers, T. C. (2023) Non-local thermodynamic equilibrium analysis of the methylidyne radical molecular lines in metal-poor stellar atmospheres. A&A, 670, A25. https://doi.org/10.1051/0004-6361/202245503.

Purandardas, M. and Goswami, A. (2021a) Chemical analysis of two extremely metal-poor stars HE 2148–2039 and HE 2155–2043. ApJ, 912(1), 74. https://doi.org/10.3847/1538-4357/abec45.

Purandardas, M. and Goswami, A. (2021b) Observational evidence points at AGB stars as possible progenitors of CEMP-*s* and CEMP-r/s stars. ApJ, 922(1), 28. https://doi.org/10.3847/1538-4357/ac1d4d.

Purandardas, M., Goswami, A., Goswami, P. P., Shejeelammal, J. and Masseron, T. (2019) Chemical analysis of CH stars – III. Atmospheric parameters and elemental abundances. MNRAS, 486(3), 3266–3289. https://doi.org/10.1093/mnras/stz759.

Qian, Y.-Z. (2022) Probing massive star nucleosynthesis with data on metal-poor stars and the solar system. EPJWC, 260, 09001. https://doi.org/10.1051/epjconf/202226009001.

Rossi, S., Beers, T. C. and Sneden, C. (1999) Carbon abundances for metal-poor stars based on medium-resolution spectra. In The Third Stromlo Symposium: The Galactic Halo, edited by Gibson, B. K., Axelrod, R. S. and Putman, M. E., vol. 165 of *ASPC*, pp. 264–268.

Salvadori, S., Schneider, R. and Ferrara, A. (2007) Cosmic stellar relics in the Galactic halo. MNRAS, 381(2), 647–662. https://doi.org/10.1111/j.1365-2966.2007.12133.x.

Shejeelammal, J. and Goswami, A. (2021) Probing the nucleosynthetic contribution of low-metallicity, low-mass star companions of CEMP stars. ApJ, 921(1), 77. https://doi.org/10.3847/1538-4357/ac1ac9.

Shejeelammal, J. and Goswami, A. (2022) Spectroscopic study of four metal-poor carbon stars from the Hamburg/ESO survey: On confirming the low-mass nature of their companions. ApJ, 934(2), 110. https://doi.org/10.3847/1538-4357/ac7aac.

Shejeelammal, J., Goswami, A., Goswami, P. P., Rathour, R. S. and Masseron, T. (2020) Characterizing the companion AGBs using surface chemical composition of barium stars. MNRAS, 492(3), 3708–3727. https://doi.org/10.1093/mnras/stz3518.

Shejeelammal, J., Goswami, A. and Shi, J. (2021) HCT/HESP study of two carbon stars from the LAMOST survey. MNRAS, 502(1), 1008–1025. https://doi.org/10.1093/mnras/staa3892.

Skúladóttir, Á., Hansen, C. J., Choplin, A., Salvadori, S., Hampel, M. and Campbell, S. W. (2020) Neutron-capture elements in dwarf galaxies. II. Challenges for the *s*- and *i*-processes at low metallicity. A&A, 634, A84. https://doi.org/10.1051/0004-6361/201937075.

Spite, M., Caffau, E., Bonifacio, P., Spite, F., Ludwig, H. G., Plez, B. and Christlieb, N. (2013) Carbon-enhanced metal-poor stars: the most pristine objects? A&A, 552, A107. https://doi.org/10.1051/0004-6361/201220989.

Starkenburg, E., Shetrone, M. D., McConnachie, A. W. and Venn, K. A. (2014) Binarity in carbon-enhanced metal-poor stars. MNRAS, 441(2), 1217–1229. https://doi.org/10.1093/mnras/stu623.

Tominaga, N., Iwamoto, N. and Nomoto, K. (2014) Abundance profiling of extremely metal-poor stars and supernova properties in the early universe. ApJ, 785(2), 98. https://doi.org/10.1088/0004-637X/785/2/98.

Umeda, H. and Nomoto, K. (2003) First-generation black-hole-forming supernovae and the metal abundance pattern of a very iron-poor star. Natur, 422(6934), 871–873. https://doi.org/10.1038/nature01571.

Umeda, H. and Nomoto, K. (2005) Variations in the abundance pattern of extremely metal-poor stars and nucleosynthesis in population III supernovae. ApJ, 619(1), 427–445. https://doi.org/10.1086/426097.

van Raai, M. A., Lugaro, M., Karakas, A. I., García-Hernández, D. A. and Yong, D. (2012) Rubidium, zirconium, and lithium production in intermediate-mass asymptotic giant branch stars. A&A, 540, A44. https://doi.org/10.1051/0004-6361/201117896.

Wallerstein, G., Iben, J., Icko, Parker, P., Boesgaard, A. M., Hale, G. M., Champagne, A. E., Barnes, C. A., Käppeler, F., Smith, V. V., Hoffman, R. D., Timmes, F. X., Sneden, C., Boyd, R. N., Meyer, B. S. and Lambert, D. L. (1997) Synthesis of the elements in stars: forty years of progress. RvMA, 69(4), 995–1084. https://doi.org/10.1103/RevModPhys.69.995.

Yong, D., Norris, J. E., Bessell, M. S., Christlieb, N., Asplund, M., Beers, T. C., Barklem, P. S., Frebel, A. and Ryan, S. G. (2013a) The most metal–poor stars. III. The metallicity distribution function and carbon-enhanced metal-poor fraction. ApJ, 762(1), 27. https://doi.org/10.1088/0004-637X/762/1/27.

Yong, D., Norris, J. E., Bessell, M. S., Christlieb, N., Asplund, M., Beers, T. C., Barklem, P. S., Frebel, A. and Ryan, S. G. (2013b) The most metal-poor stars. II. Chemical abundances of 190 metal-poor stars including 10 new stars with [Fe/H] ≤ -3.5. ApJ, 762(1), 26. https://doi.org/10.1088/0004-637X/762/1/26.

Yoon, J., Beers, T. C., Dietz, S., Lee, Y. S., Placco, V. M., Da Costa, G., Keller, S., Owen, C. I. and Sharma, M. (2018) Galactic archeology with the AEGIS survey: The evolution of carbon and iron in the Galactic halo. ApJ, 861(2), 146. https://doi.org/10.3847/1538-4357/aaccea.

Yoon, J., Beers, T. C., Placco, V. M., Rasmussen, K. C., Carollo, D., He, S., Hansen, T. T., Roederer, I. U. and Zeanah, J. (2016) Observational constraints on first-star nucleosynthesis. I. Evidence for multiple progenitors of CEMP-no stars. ApJ, 833(1), 20. https://doi.org/10.3847/0004-637X/833/1/20.

Yoon, J., Beers, T. C., Tian, D. and Whitten, D. D. (2019) Origin of the CEMP-no group morphology in the Milky Way. ApJ, 878(2), 97. https://doi.org/10.3847/1538-4357/ab1ead.

Yoon, J., Whitten, D. D., Beers, T. C., Lee, Y. S., Masseron, T. and Placco, V. M. (2020) Identification of a Group III CEMP-no star in the dwarf spheroidal galaxy Canes Venatici I. ApJ, 894(1), 7. https://doi.org/10.3847/1538-4357/ab7daf.

York, D. G., Adelman, J., Anderson, J., John E., Anderson, S. F., Annis, J., Bahcall, N. A., Bakken, J. A., Barkhouser, R., Bastian, S., Berman, E., Boroski, W. N., Bracker, S., Briegel, C., Briggs, J. W., Brinkmann, J., Brunner, R., Burles, S., Carey, L., Carr, M. A., Castander, F. J., Chen, B., Colestock, P. L., Connolly, A. J., Crocker, J. H., Csabai, I., Czarapata, P. C.,

Davis, J. E., Doi, M., Dombeck, T., Eisenstein, D., Ellman, N., Elms, B. R., Evans, M. L., Fan, X., Federwitz, G. R., Fiscelli, L., Friedman, S., Frieman, J. A., Fukugita, M., Gillespie, B., Gunn, J. E., Gurbani, V. K., de Haas, E., Haldeman, M., Harris, F. H., Hayes, J., Heckman, T. M., Hennessy, G. S., Hindsley, R. B., Holm, S., Holmgren, D. J., Huang, C.-h., Hull, C., Husby, D., Ichikawa, S.-I., Ichikawa, T., Ivezić, Ž., Kent, S., Kim, R. S. J., Kinney, E., Klaene, M., Kleinman, A. N., Kleinman, S., Knapp, G. R., Korienek, J., Kron, R. G., Kunszt, P. Z., Lamb, D. Q., Lee, B., Leger, R. F., Limmongkol, S., Lindenmeyer, C., Long, D. C., Loomis, C., Loveday, J., Lucinio, R., Lupton, R. H., MacKinnon, B., Mannery, E. J., Mantsch, P. M., Margon, B., McGehee, P., McKay, T. A., Meiksin, A., Merelli, A., Monet, D. G., Munn, J. A., Narayanan, V. K., Nash, T., Neilsen, E., Neswold, R., Newberg, H. J., Nichol, R. C., Nicinski, T., Nonino, M., Okada, N., Okamura, S., Ostriker, J. P., Owen, R., Pauls, A. G., Peoples, J., Peterson, R. L., Petravick, D., Pier, J. R., Pope, A., Pordes, R., Prosapio, A., Rechenmacher, R., Quinn, T. R., Richards, G. T., Richmond, M. W., Rivetta, C. H., Rockosi, C. M., Ruthmansdorfer, K., Sandford, D., Schlegel, D. J., Schneider, D. P., Sekiguchi, M., Sergey, G., Shimasaku, K., Siegmund, W. A., Smee, S., Smith, J. A., Snedden, S., Stone, R., Stoughton, C., Strauss, M. A., Stubbs, C., SubbaRao, M., Szalay, A. S., Szapudi, I., Szokoly, G. P., Thakar, A. R., Tremonti, C., Tucker, D. L., Uomoto, A., Vanden Berk, D., Vogeley, M. S., Waddell, P., Wang, S.-i., Watanabe, M., Weinberg, D. H., Yanny, B., Yasuda, N. and SDSS Collaboration (2000) The Sloan Digital Sky Survey: Technical summary. AJ, 120(3), 1579–1587. https://doi.org/10.1086/301513.

Zepeda, J., Beers, T. C., Placco, V. M., Shank, D., Gudin, D., Hirai, Y., Mardini, M., Pifer, C., Catapano, T. and Calagna, S. (2023) Chemodynamically tagged groups of CEMP stars in the halo of the Milky Way. I. Untangling the origins of CEMP-*s* and CEMP-no stars. ApJ, 947(1), 23. https://doi.org/10.3847/1538-4357/acbbcc.

Zhao, G., Zhao, Y.-H., Chu, Y.-Q., Jing, Y.-P. and Deng, L.-C. (2012) LAMOST spectral survey — An overview. RAA, 12(7), 723–734. https://doi.org/10.1088/1674-4527/12/7/002.